



An intelligent control strategy of fractional short circuit current maximum power point tracking technique for photovoltaic applications

Hadeed Ahmed Sher,^{1,a)} Ali F. Murtaza,^{2,4} Abdullah Noman,¹
Khaled E. Addoweesh,¹ and Marcello Chiaberge³

¹*Department of Electrical Engineering, King Saud University, Riyadh 11421, Saudi Arabia*

²*Department of Mechanical and Aerospace Engineering, Politecnico di Torino, Turin, Italy*

³*Department of Electronics and Telecommunication Engineering, Politecnico di Torino, Turin, Italy*

⁴*Department of Electrical Engineering, University of Central Punjab, Lahore, Pakistan*

(Received 17 October 2014; accepted 17 January 2015; published online 29 January 2015)

This paper presents an improved Fractional Short Circuit Current (FSCC) Maximum Power Point Tracking (MPPT) technique in which an additional control loop is used to find the proper moment to measure the SCC. The target is to reduce the power losses in MPPT process that occur as a result of intermittent time based short circuit current measurements. The proposed modification enables the conventional FSCC MPPT to decide intelligently about the measurement of SCC thus reduces the number of times the photovoltaic (PV) module is isolated from the load. Although number of algorithms for tracking MPPT has been reported, the proposed method suits well for low cost PV applications. A Matlab/Simulink based model is employed to test the functional abilities of the proposed method. The comparison of the proposed method and conventional time based FSCC method is also presented in the simulation analysis. Finally, a 130 W prototype based on the dSPACE DS1104 controller and experimental results are presented to verify the effectiveness of the proposed method. The technique is verified under uniform shading conditions. The results show satisfactory performance against test conditions. © 2015 AIP Publishing LLC. [<http://dx.doi.org/10.1063/1.4906982>]

I. INTRODUCTION

The threat of depleting conventional energy sources has made a tremendous impact on the search for Renewable Energy (RE) sources like solar photovoltaic (PV), solar thermal, wind, biomass, etc. 21st century has seen a remarkable growth in the utilization of RE sources for electric power generation. In the recent decades, the manufacturing price of solar PV based systems has substantially reduced. It is pertinent to mention that, with the advancement in PV technology, the per unit cost has also dropped.¹ This boosted the use of solar PV based system for energy generation, especially for domestic roof top applications. Presently, the installed capacity of solar PV systems has surpassed 100 GW.² PV system does not pose challenges to the environment and it has no greenhouse emissions, which makes it an environment friendly option for power generation. It is expected that with this pace the PV system will soon become the largest stakeholder in RE sources.³

Solar PV module is a dependent current source in which the output current depends on the amount of solar irradiation falling on its surface. Because the building block of PV panel is a semiconductor, the nature of PV modules is non-linear and therefore, on the I-V locus of an unshaded single PV module, there is only one unique point of maximum power. This makes PV systems special as compared to the conventional linear electricity sources. In order to track

^{a)} Author to whom correspondence should be addressed. Electronic mail: hsher@ksu.edu.sa

the Maximum Power Point (MPP), special algorithms are required that force the system to operate close to the MPP. These algorithms are known as MPP tracking (MPPT) techniques. In the wake of nonlinear characteristics of the PV module, MPPT technique is a basic requirement for a PV system. In literature, dozens of methods have been reported to track the MPP.⁴ However, the following methods are widely adopted for research activities:⁴

- Perturb & Observe (P&O)
- Incremental Conductance (InC)
- Fractional Open Circuit Voltage (FOCV)
- Fractional Short Circuit Current (FSCC)

The above mentioned methods can be classified based on the isolation of the PV module. Thus, in the above mentioned methods the P&O and InC can be classified as online MPPT techniques, because they track the MPP without detaching the panel from the system. These two techniques are, however, difficult and complex as far as implementation is concerned. Although they do not incur power loss as a result of PV module isolation, but suffer power loss due to oscillation of operating point around MPP. This loss due to power oscillations can be controlled by varying the step size for each perturbation. On the other side, the FOCV and FSCC isolate the PV module for finding the MPP and thus considered as offline techniques.⁵ Both the offline MPPT methods have an advantage that they are very simple to implement and they rapidly converge to the approximated MPP. They can be implemented using analog or digital methods. The disadvantage with them, however, is that they suffer from power loss as an obvious result of periodic isolation of the PV array. To solve the issue of periodic measurement, the use of irradiance sensor for measuring the irradiance can be helpful.⁶ Using this sensor, the system can decide about the measurement of the short circuit current at desired instants. However, the use of sensor for irradiation measurement increases the cost of the system and it is also not feasible to install expensive irradiance sensors on each and every module of a solar PV plant. Time based measurements are reported in literature for offline MPPT techniques. The work presented in Ref. 7 is about FOCV MPPT where the PV array is isolated on fixed intervals to measure the open circuit voltage. Similarly, the work of Ref. 8 is also a periodic measurement for MPPT. The comparison of different MPPT techniques is performed by Refs. 9 and 10, in which the implementation of FSCC MPPT is time based and every 3 sec the short circuit measurement was taken, hence leading to an ample power loss throughout the course of the day.

In this paper, we are presenting a solution to the above mentioned shortcomings of offline MPPT methods. The proposed method is able to decide intelligently when to isolate the PV array and can be implemented on FOCV and FSCC. In this paper the proposed method is executed for FSCC MPPT only because it has more accuracy than the FOCV.¹¹ It will be shown in the coming section that the current of the PV module depends on the light falling on the surface of the module. The effect of temperature on the value of current is minimal. Therefore, the proposed strategy revolves around the current sensing and recording in two modes. First, to measure the short circuit current of PV module and second, to measure the current of PV module with load connected. The proposed method monitors continuously the difference between the recorded value of the short circuit current (I_{sc}) and the photovoltaic current (I_{pv}). As discussed above, the proposed method is not time based measurement of short circuit current (I_{sc}); therefore, the decision about next value of the I_{sc} measurement is based entirely on the difference of I_{sc} and I_{pv} . Thus, the proposed method does not require irradiance sensor and it modifies the FSCC MPPT technique such that the PV array is isolated to measure I_{sc} , only when there is a sufficient change in weather conditions. The additional control loop proposed in this paper first sets the limit and then calculates the difference between I_{sc} and I_{pv} and takes the decision about the measurement of short circuit current. The difference between I_{sc} and I_{pv} is based on the data sheet of the PV module. It is a constant and can be calculated using the datasheet of PV module. The proposed modification in the FSCC algorithm is modeled and tested using Matlab/Simulink and experimentally verified using dSPACE DS1104 based embedded interface.

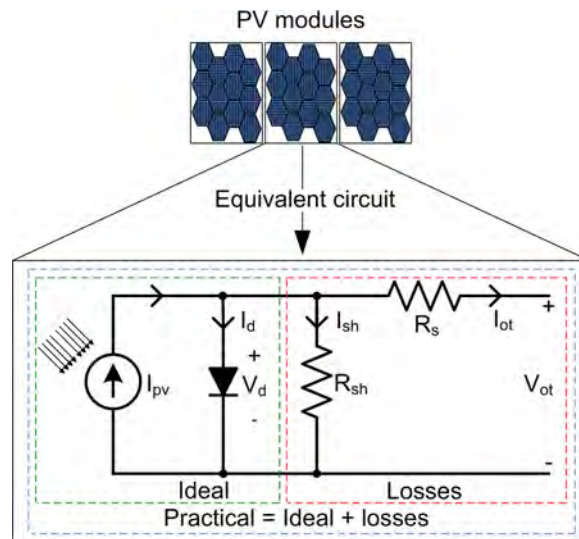


FIG. 1. Equivalent circuit of a PV cell.

II. MODELING OF SOLAR PV MODULE

PV systems essentially convert light into electrical current. The amount of current generated depends on the efficiency, surface area, and amount of irradiation falling on the module. The single diode model of a single PV module is shown in Fig. 1.¹²

In this figure,

- I_{pv} is the photovoltaic current which is directly proportional to the amount of irradiation falling on the PV module
- I_d is the single exponential junction current and is given by $I_d = I_o(e^{qV_d/akT} - 1)$, where
 - I_o = Leakage current of the diode D
 - q = Charge on electron
 - k = Boltzmann constant
 - T = Temperature in K
 - a = Diode ideality constant

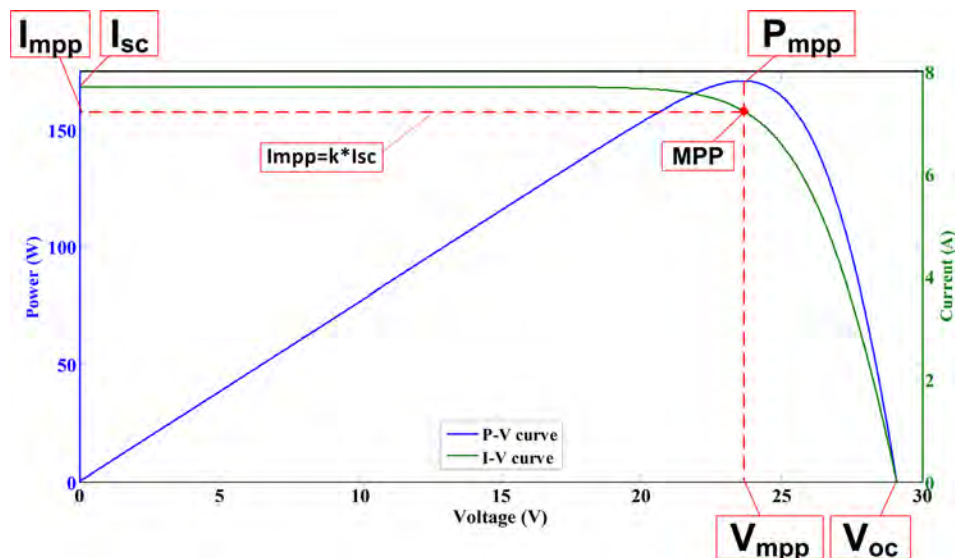


FIG. 2. Characteristics curve of a typical PV cell.

- I_{ot} is the output current which is given by $I_{ot} = I_{pv} - I_d - V_d/R_{sh}$
- V_{ot} is the output voltage given by $V_{ot} = V_d - R_s I$.

By simulating the circuit according to the equations mentioned above, the I-V and P-V characteristics are obtained that are shown in Fig. 2. As seen in Fig. 2, there is a single operating point with maximum power, provided that the environmental conditions are constant. However, according to the governing equations of the equivalent circuit the behavior of the circuit is non-linear. Therefore, by varying irradiance the value of the short circuit current changes proportionally, while the value of the open circuit voltage changes with change in temperature. Thus, the changing weather conditions lead theoretically, to the infinite possibilities of maximum power point. Figure 3 shows the effect of varying environmental conditions on MPP. Keeping into consideration the effect of temperature (T) and irradiance (G), the computation of I_{sc} , V_{oc} and P_m can be performed using the following equations:⁶

$$I_{sc}(G, T) = I_{sc}(STC) \times G/1000 \times (1 + \alpha I_{sc} \Delta T), \quad (1)$$

$$V_{oc}(T) = V_{oc}(STC) \times (1 + \beta V_{oc} \Delta T), \quad (2)$$

$$P_m(G, T) = P_m(STC) \times G/1000 \times (1 + \gamma p \Delta T), \quad (3)$$

$$\eta = P_m/GA = P_m(STC) \times (1 + \gamma p \Delta T)/A. \quad (4)$$

In the above equations, STC is standard testing condition, i.e., 1000 W/m^2 at 25°C , while $\Delta T = T_c - 25^\circ\text{C}$.

The above equations show that the change of radiance has a very small effect on the value of V_{oc} and the temperature difference has a minor change in the value of I_{sc} . In this paper, PV module model number BP3115 is used for simulation as well as the experimental work. The characteristics of this module, under standard testing conditions of 1000 W/m^2 at 25°C are given in Table I.¹⁴

The characteristic curves, derived through simulation, for this module is shown in Figs. 4 and 5. Where Fig. 4 shows the P-V curve under changing irradiation and Fig. 5 is the behavior of the P-V curve under varying temperature.

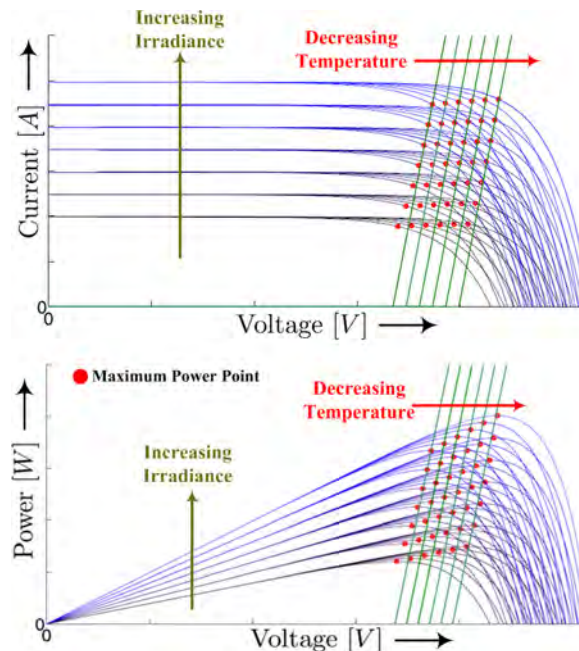


FIG. 3. Variation of maximum power point.¹³

TABLE I. PV Module parameters.

Power at MPP (P_{mpp})	115 W
Voltage at MPP (V_{mpp})	17.1 V
Current at MPP (I_{mpp})	6.7 A
Open circuit voltage (V_{oc})	21.8 V
Short circuit current (I_{sc})	7.5 A
Temperature coefficient of I_{sc}	$0.065 \pm 0.015\%/^{\circ}\text{C}$
Temperature coefficient of power	$-(0.5 \pm 0.05)\%/^{\circ}\text{C}$

III. FRACTIONAL SHORT CIRCUIT CURRENT MPPT

FSCC is an unsophisticated but a swift technique of tracking the MPP. To track the power, this MPPT technique requires the value of SCC by isolating the PV array. The MPPT calculated using this technique is based on Eq. (5) which is an approximation, hence this method does not operate on true MPPT. Nevertheless, the simplicity of this technique makes it suitable for use in small scale cheap applications. This method is suitable to be implemented by using either the analog or the digital mode. The basic outline of this technique follows that the current at MPP (I_{mpp}) is closely located near the short circuit current I_{sc} . Therefore, the operating point can be reached by multiplying I_{sc} by the factor k as given below:

$$I_{mpp} \approx k I_{sc}. \quad (5)$$

The constant “ k ” can be easily calculated from the specifications of the PV module and it is always less than 1. The constant k is a fixed value and therefore, can be used as a fixed entity in the algorithm. Typically the value of k is in between 0.85 and 0.95.⁴ FSCC MPPT needs only a current sensor and therefore it is less expensive and easy to implement. The disadvantage includes the periodic loss of power while measuring the short circuit current.

IV. PROPOSED TECHNIQUE

The modified algorithm of the FSCC MPPT is shown in Fig. 6. It has two loops, i.e., normal loop and I_{pv} loop. The flow chart shown in Fig. 6 has two inputs that are the short circuit current I_{sc} and the current of PV array I_{pv} .

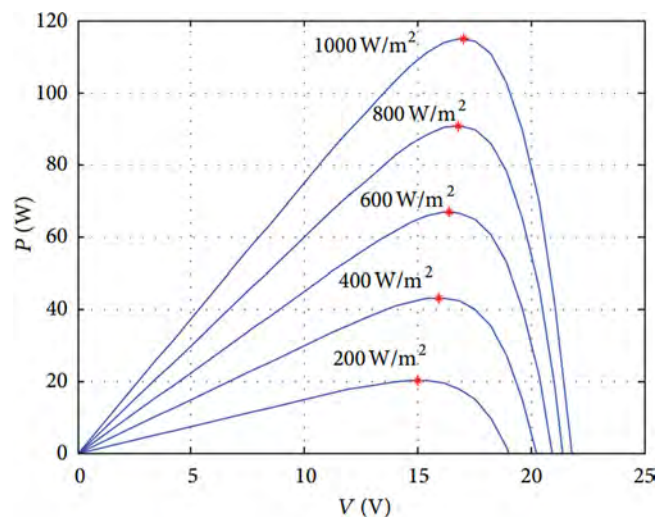


FIG. 4. Simulation of P-V curve of PV module under changing irradiance.

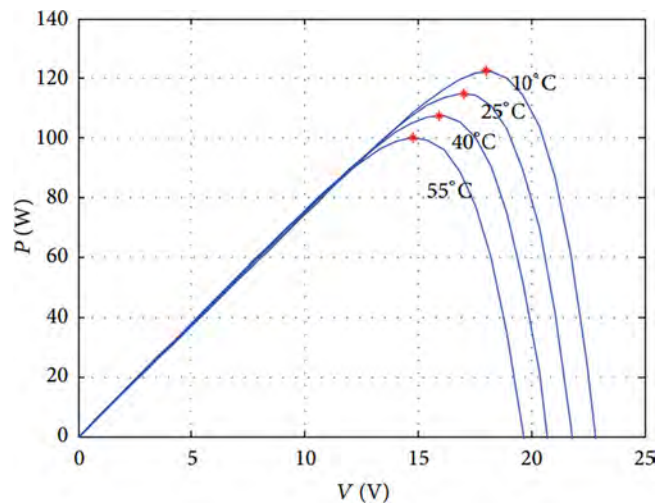


FIG. 5. Simulation of P-V curve of PV module under changing temperature.

Because the change in temperature is slow and less as compared with the irradiance, and because the effect of temperature on the value of short circuit current is negligible, the effect of temperature on the system is not taken into consideration. The functionality of this flowchart is explained below.

A. Normal loop

The system starts its work with this loop. Every time when the system is started, the PV array is isolated from the system and short circuit current I_{sc} is measured and stored in the

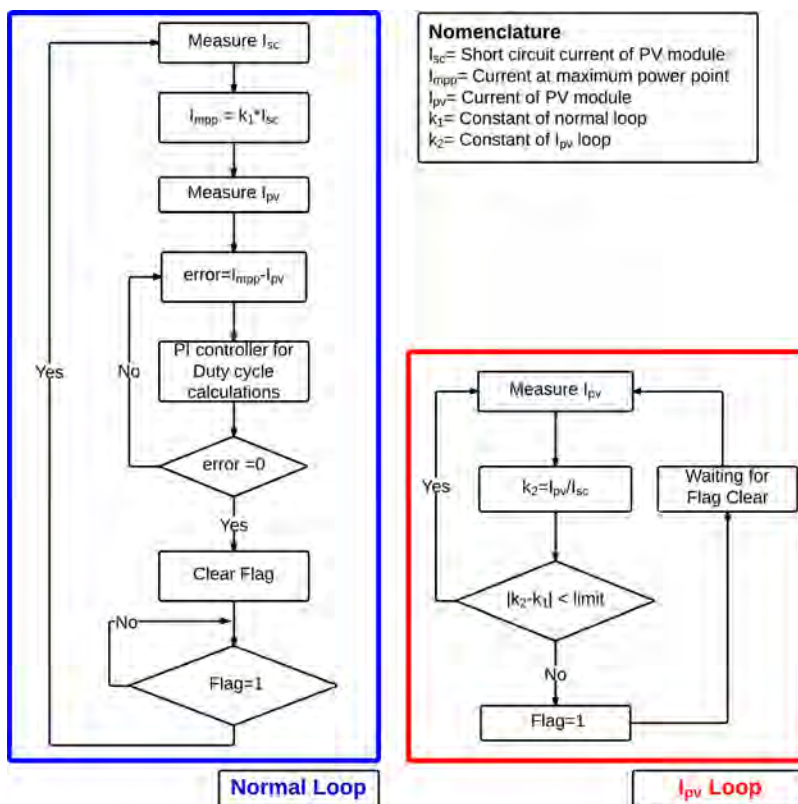


FIG. 6. Flow chart of the proposed technique.

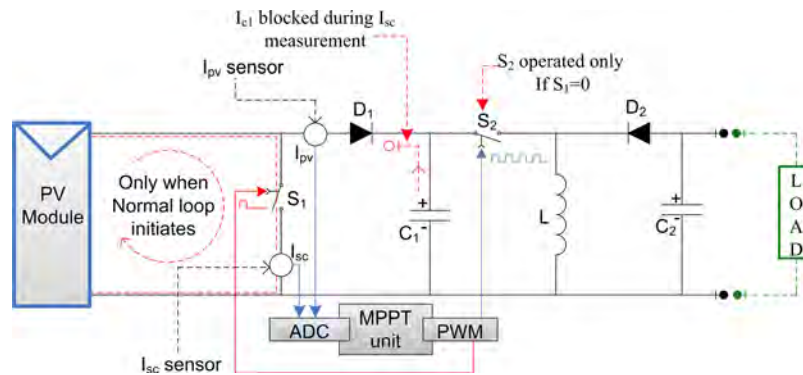


FIG. 7. Circuit operation during normal loop operation.

memory. This process is shown in Fig. 7. During the initialization process of this loop, only the red part of the circuit is active. Later, in order to estimate the operating point for maximum power, the value of I_{sc} is multiplied with “ k_1 .” The value of normal loop constant “ k_1 ” varies for different modules and should be calculated according to the data sheet of the PV module. The calculated operating point value is then compared with the I_{pv} and the error is measured and fed to the PI controller for duty cycle calculation. The duty cycle is then adjusted by the PI controller until the error is zero. Once the error is zero the loop clears the flag. It then monitors the flag continuously. As soon as the flag becomes equal to 1, the loop starts the whole process again. The flag is set by the I_{pv} loop which is explained below.

B. I_{pv} Loop

The main task of this loop is to set/reset the flag based on the sampled value of I_{pv} . It has a constant “ k_2 ” whose value is updated by the discrete monitoring of “ I_{pv} ” and the stored value of “ I_{sc} .” This constant k_2 is then compared with the constant of normal loop k_1 . If it is less than the limit, then the process is repeated. The limit defines the sensitivity of the system, lower value of the limit means more measurement of I_{sc} and higher value means less short circuit current measurements. This means that if the limit is very small then system will experience more I_{sc} measurements and hence more power loss and if the limit is large then the system may work far from the expected MPP. By hit and trial error, the optimized value of this limit for the simulation and experimental setup is set at 0.02. If the difference between the two constants surpassed this limit, then the algorithm sets the flag to 1. This reinstates the normal loop and the fresh value of I_{sc} is measured. This loop then waits until the flag is cleared by the normal loop. Once the flag is clear this loop will again follow its routine.

V. SIMULATION RESULTS AND ANALYSIS

To verify the effectiveness of the proposed technique, simulation is performed using Matlab/Simulink as shown in Fig. 8. The parameters of the simulation setup are given below.

- PV module: Specifications are given in Table I.
- DC-DC converter: Buck-boost converter with following parameters
 - Input capacitor $C_1 = 1000 \mu\text{F}$
 - Output capacitor $C_2 = 1000 \mu\text{F}$
 - Inductor $L = 0.5 \text{ mH}$
 - Resistive load $= 5 \Omega$
 - Switching frequency $= 25 \text{ kHz}$.

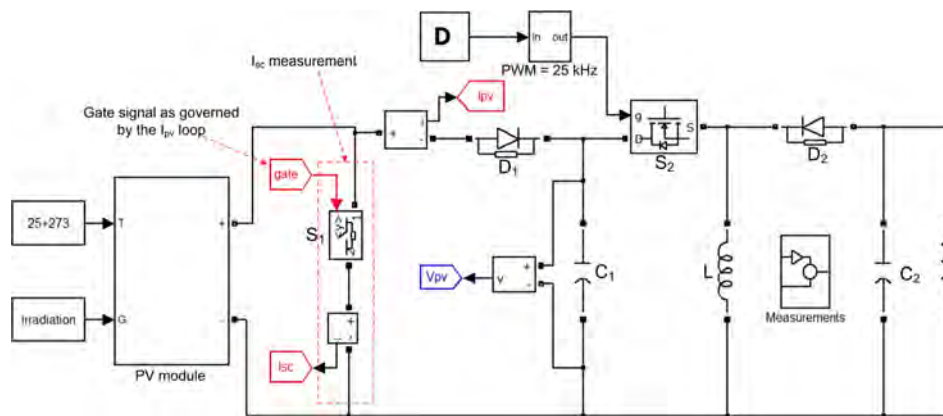


FIG. 8. Simulation setup.

A. Simulation results

The proposed algorithm is tested under steady and dynamic weather conditions. For comparison, the proposed FSCC MPPT is compared with a conventional time based FSCC method. Both the algorithms are applied to the buck-boost converter of the same rating. It is pertinent to mention here that for the simulation of time based algorithm measurement of I_{sc} is performed every 0.01 s. This can be considered a fair approximation when we superimpose the total simulation time of 0.1 s over a full day operation.

Steady weather condition: A steady weather condition is realized by setting the system according to the standard testing conditions of solar PV modules. For this the irradiance is set at 1000 W/m^2 at 25°C . At start due to the measurement of I_{sc} the power is zero, which later on shows a good steady performance. Figure 9 shows the current, voltage, and power extracted from the PV module using the proposed and conventional time based FSCC method. For the proposed method, during the steady weather condition, there is no need of intermittent measurement of short circuit current. The measurements at the start of the process are used in the whole course of MPPT. However, for the conventional time based FSCC, the samples are taken irrespective of the environmental condition.

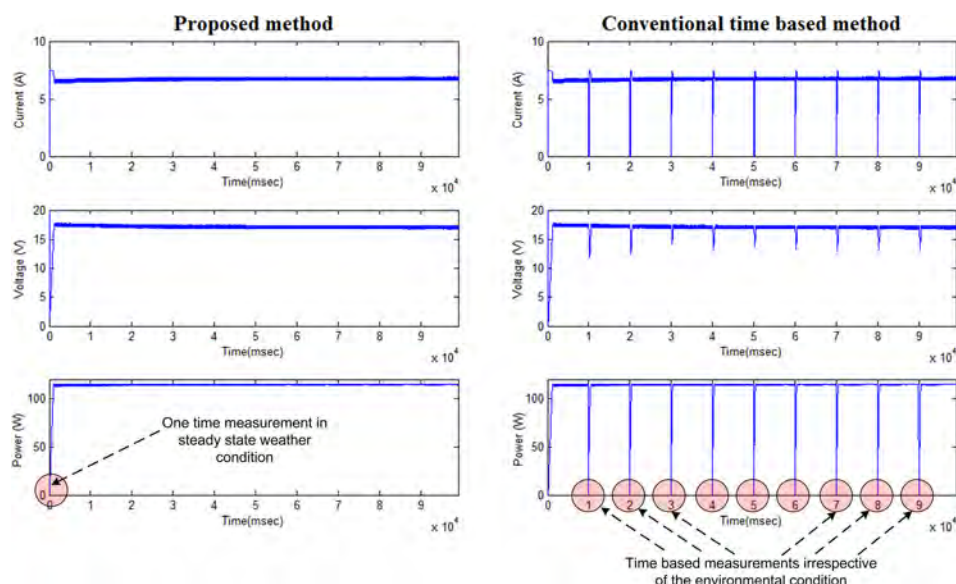


FIG. 9. Result of the proposed technique under steady weather condition.

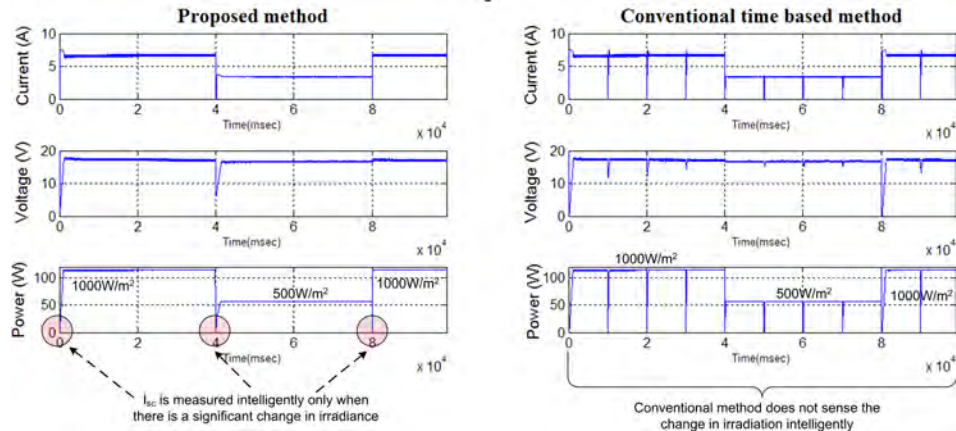


FIG. 10. Dynamic weather condition—Scenario I.

Dynamic weather condition: In order to see the performance of the proposed scheme under changing environmental condition, two scenarios are examined that are given below.

Scenario I: In this scenario, the irradiation is decreased from the 1000 W/m² to 500 W/m² and then back to 1000 W/m². The temperature is kept constant at 25 °C. The comparative results are shown in Fig. 10.

Scenario II: In this scenario, the irradiation is abruptly changed (1000 W/m² to 700 W/m² and then 500 W/m²) such that the irradiation changes in between the instants of time based measurement. This rapid change in environmental condition is applied to see the behavior of the proposed technique as well as the conventional time based method. It is visible from the results shown in Fig. 11 that at time 1.5 sec, for the conventional time based method, the power is considerably lost because the sample taken at time $t = 1$ is not valid for the system. The conventional time based method reaches again to a steady power level after the next sample is taken at $t = 2$.

For comparison, the ideal values of MPP at various levels of irradiance are tabulated in Table II.

B. Simulation analysis

The results presented above have some attributes that need to analyze. First, the value of constant k_2 defines sensitivity. Very small values of k_2 imply a more frequent measurement of

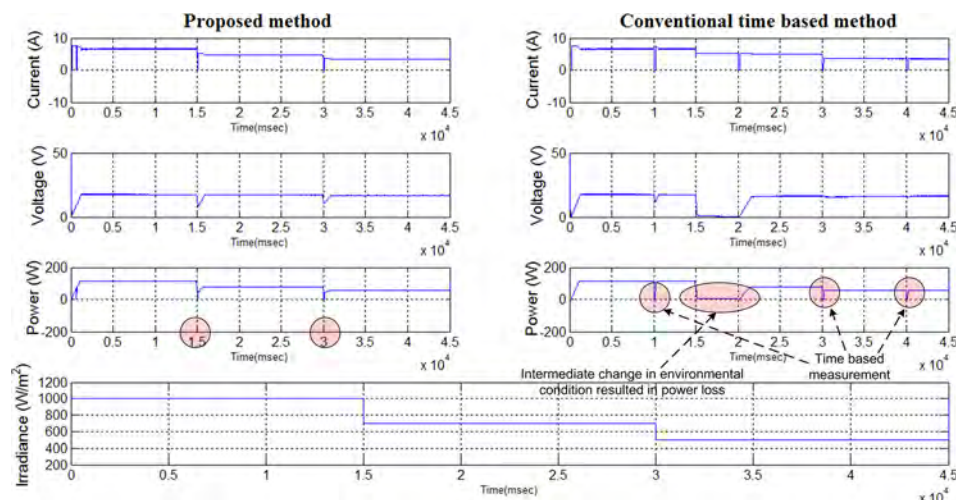


FIG. 11. Dynamic weather condition—Scenario II.

TABLE II. Ideal values of MPP at different irradiation levels.

Irradiation (W/m ²)	Maximum power (W)
500	56.73
550	62.63
600	68.53
650	74.4
700	80.2
750	86.15
800	91.9
850	97.8
900	103.6
950	109.3
1000	115

I_{sc} and vice versa. Therefore, the sensitivity must be calculated by empirically adjusting the value of k_2 . The percentage tracking efficiency for the proposed MPPT can be calculated by using the following equation:¹⁵

$$\eta = \frac{\int_{t_1}^{t_2} P_{mpp} dt}{\int_{t_1}^{t_2} P_i dt}. \quad (6)$$

In Eq. (6), t_1 is the starting time and t_2 is the ending time of simulation. Using Eq. (6), the tracking efficiency for the steady state weather condition is 98.6%. For dynamic weather condition, the data sampling is performed on Fig. 10 and calculated to be 97.49%. Table III shows the energy comparison using the conventional time based FSCC method and the proposed intelligent method over each simulation time. The difference seems small but this is because the total simulation time is less than a second.

VI. EXPERIMENTAL VERIFICATION

An experimental setup was established to verify the proposed technique practically. A buck-boost converter similar to the simulation setup was engineered for the testing of the proposed technique. For sensing the current, a hall effect current sensor was used. An additional diode (D_1) was connected between PV module and the input capacitor. During the short circuit measurement, this diode (D_1) prevents the discharge of input capacitor (C_1) through the short circuit path. The interfacing of Simulink with the real time hardware setup was accomplished with a dSPACE DS1104 based embedded card. Figure 12 shows the block diagram of the MPPT hardware setup using dSPACE real-time control. While Fig. 13 shows the actual hardware setup. Each section of Fig. 13 is marked and its detail is given in Table IV. It should be noted that all voltage measurements are made using conventional potential divider networks and current measurements using hall effect current sensor model No. LTS 25-NP. It is also pertinent to mention that the irradiation sensor as seen in section H of Fig. 13 is used only to

TABLE III. Energy comparison.

Weather condition	Proposed MPPT (J)	Conventional time based method (J)
Steady	11.4	11
Dynamic Scenario I	11.3	11.08
Dynamic Scenario II	3.6	3.1

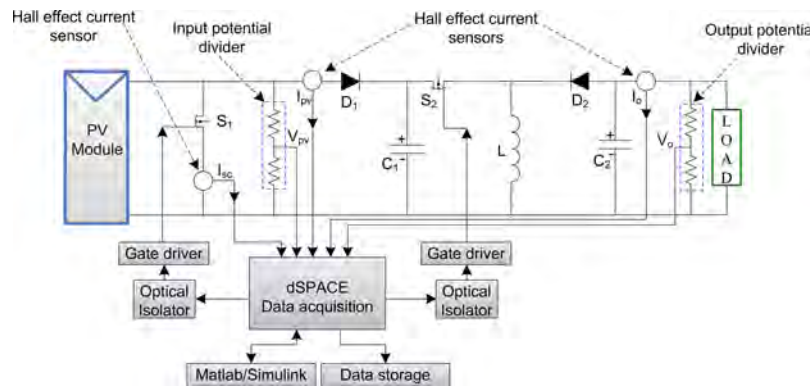


FIG. 12. Block diagram of the hardware setup.

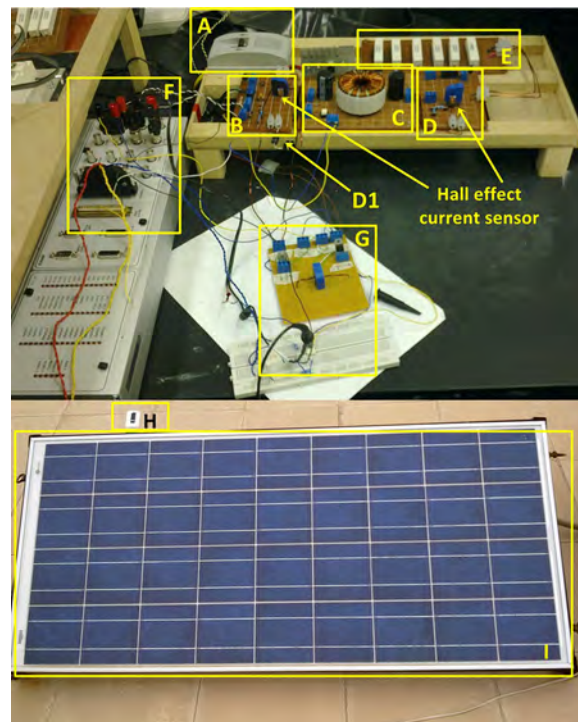


FIG. 13. Hardware Prototype model (see Table IV for details).

TABLE IV. Section detail of prototype model.

A	Input circuit breaker
B	Input transducers for V_{pv} and I_{pv} measurements.
C	Buck-boost DC-DC converter C_1 , L and C_2 can be seen
D	Output transducers for V_o and I_o measurements
D1	Diode to block the discharge of C_1
E	Load (Resistor bank)
F	dSPACE R&D controller board for data acquisition
G	Arrangement for I_{sc} measurement
H	Sensor for measuring irradiation
I	Solar module model No. BP3115

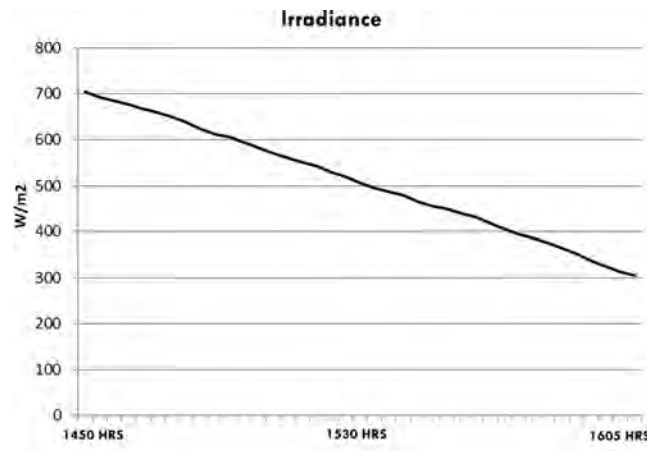
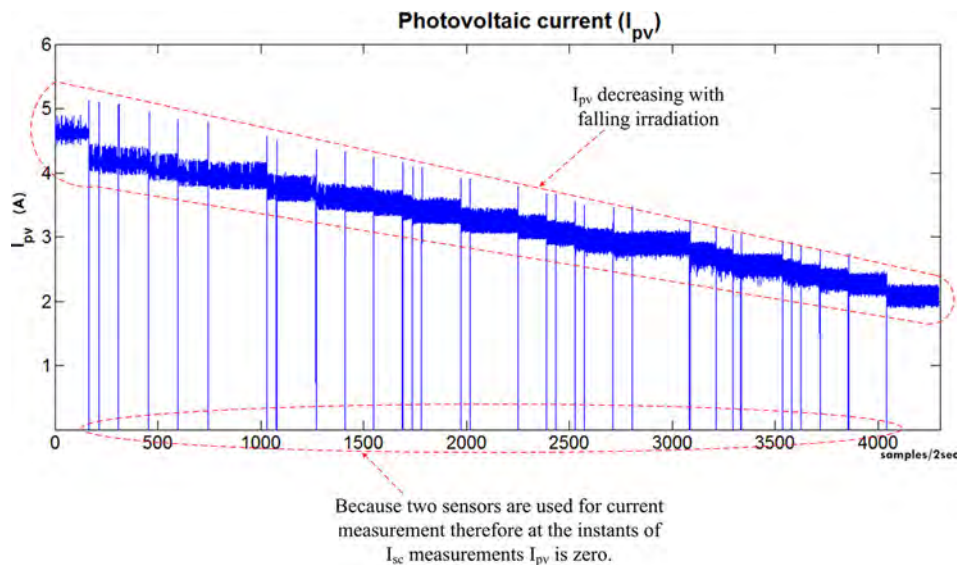


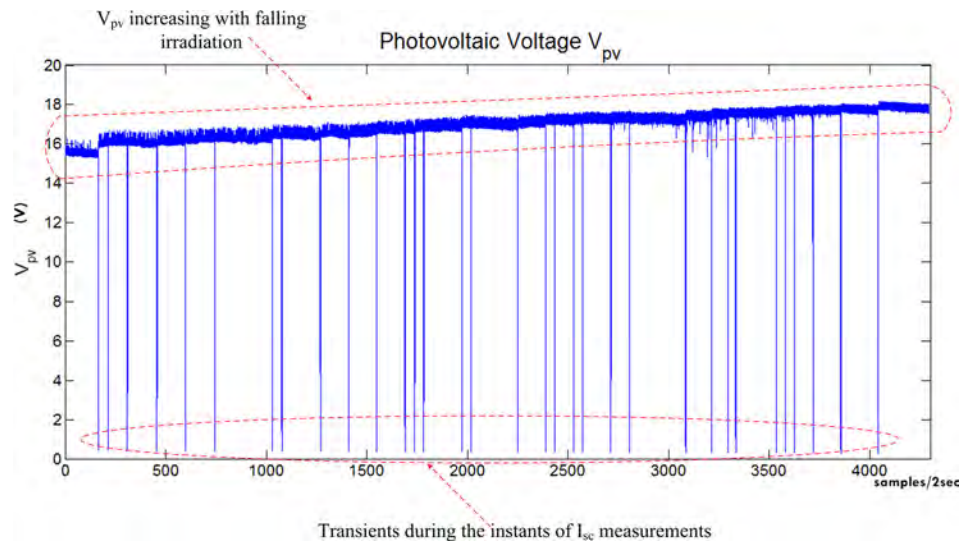
FIG. 14. Irradiance data for experiment duration.

gather the irradiation values. It has not been incorporated as part of the algorithm verification. The signal applied to a dSPACE A/D channel should be within the range of -10 V to $+10$ V. A signal of $+10$ V gives an internal value of 1; therefore, a gain block with a value of 10 is added in series with the signal flow. The low pass filters are used to remove unwanted switching noise. The output signal of the MPPT algorithm is then applied to the Pulse Width Modulation (PWM) block which is used to generate the required switching signal. The PWM channel is connected to a gate driver that drives the power MOSFET.

VII. EXPERIMENTAL RESULTS

The experiment was conducted after the mid noon from 1455 HRS till 1605HRS. The irradiation curve is shown in Fig. 14. Figure 15 shows the photovoltaic current and Fig. 16 shows the voltage of the photovoltaic module. Figure 17 shows the photovoltaic power tracked by the proposed algorithm. As shown in Fig. 17, the proposed MPPT method has tracked the maximum power effectively and accurately under changing solar irradiation.

FIG. 15. Experimental results: I_{pv} .

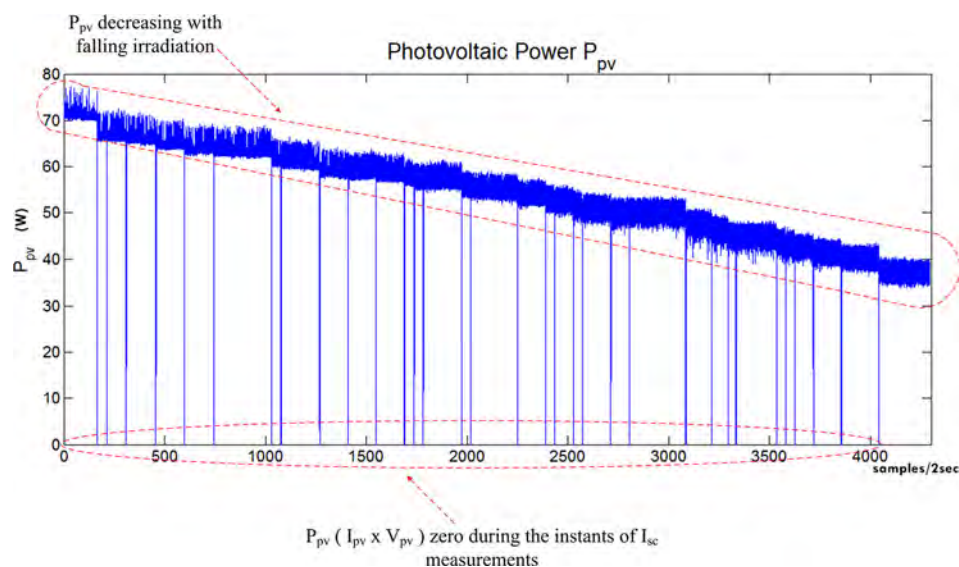
FIG. 16. Experimental results: V_{pv} .

VIII. CONCLUSION

In this paper, we have proposed an improvement in offline MPPT technique. The proposed improvement can be applied to either the FOCV or to the FSCC. Simulation as well as experimentation has been performed for FSCC MPPT. The proposed modification intelligently calculates the right time to isolate the PV panel, thus does not need the time based measurement of short circuit current. Following are the advantages of the proposed method:

- The modified control methodology eliminates the necessity of any irradiance sensor.
- Intelligent detection of change in irradiation.
- A cost effective solution for low cost solar PV applications without much compromise on energy loss.

This proposed algorithm in off-line MPPT techniques as a whole will enrich the research in the field of PV systems.

FIG. 17. Experimental results: P_{pv} .

IX. LIST OF SYMBOLS AND ABBREVIATIONS

- ADC—Analog to digital converter
- FOCV—Fractional open circuit voltage
- FSCC—Fractional short circuit current
- G —Irradiance in W/m^2
- I_{c1} —Current in input capacitor branch
- I_{mpp} —Current at maximum power point
- InC —Incremental conductance
- I_d —Single exponential junction current
- I_{ot} —Output current
- I_{pv} —Photovoltaic current
- k_1 —Constant of normal loop
- k_2 —Constant of I_{pv} loop
- MPP—Maximum power point
- MPPT—Maximum power point tracking
- P_i —Ideal power at given environmental condition
- P_{mpp} —Power at maximum power point
- P_{pv} —Photovoltaic power
- P&O—Perturb and observe
- PV—Photovoltaic
- PWM—Pulse width modulation
- RE—Renewable energy
- R_s —Series resistance
- R_{sh} —Shunt resistance
- SCC—Short circuit current
- STC—Standard testing condition, i.e., 1000 W/m^2 at 25°C
- T —Temperature in $^\circ\text{C}$
- V_{mpp} —Voltage at maximum power point
- V_{ot} —Output voltage
- V_{oc} —Open circuit voltage

ACKNOWLEDGMENTS

The authors would like to acknowledge the financial support provided by the College of Engineering Research Center and Deanship of Scientific Research at King Saud University (KSU) in Riyadh, KSA.

¹C. Emmott, B. Azzopardi, N. Espinosa, R. Garcia-Valverde, A. Urbina, J. Mutale, F. C. Krebs, and J. Nelson, "Economic assessment of solar electricity from organic photovoltaic systems," in *IET Conference on Renewable Power Generation (RPG 2011)* (2011), pp. 1–2.

²G. Masson, M. Latour, M. Reikinger, I.-T. Theologitis, and M. Papouts, "Global market outlook for photovoltaics 2013–2017," *European Photovoltaics Industry Association* (2013).

³Z. Liang, R. Guo, J. Li, and A. Q. Huang, "A high-efficiency pv module integrated dc/dc converter for pv energy harvest in freedom systems," *IEEE Trans. Power Electron.* **26**(3), pp. 897–909 (2011).

⁴T. Esram and P. L. Chapman, "Comparison of photovoltaic array maximum power point tracking techniques," *IEEE Trans. Energy Convers.* **22**(2), pp. 439–449 (2007).

⁵V. Salas, E. Olas, A. Barrado, and A. Lzaro, "Review of the maximum power point tracking algorithms for stand-alone photovoltaic systems," *Sol. Energy Mater. Sol. Cells* **90**(11), pp. 1555–1578 (2006).

⁶R. Arulmurugan and N. Suthanthiravanitha, "Improved fractional order vss inc-cond mppt algorithm for photovoltaic scheme," *Int. J. Photoenergy* **2014**, 128327.

⁷D.-Y. Lee, H.-J. Noh, D.-S. Hyun, and I. Choy, "An improved mppt converter using current compensation method for small scaled pv applications," in *Eighteenth Annual IEEE Applied Power Electronics Conference and Exposition (APEC'03)* (2003), Vol. 1, pp. 540–545.

⁸J. Ahmad, "A fractional open circuit voltage based maximum powerpoint tracker for photovoltaic arrays," in *2nd International Conference on Software Technology and Engineering (ICSTE)* (2010), Vol. 1, pp. 247–250.

⁹M. Berrera, A. Dolara, R. Faranda, and S. Leva, "Experimental test of seven widely-adopted mppt algorithms," in *IEEE Bucharest PowerTech* (2009), pp. 1–8.

- ¹⁰R. Faranda, S. Leva, and V. Maugeri, "Mppt techniques for pv systems: Energetic and cost comparison," in IEEE Power and Energy Society General Meeting—Conversion and Delivery of Electrical Energy in the 21st Century (2008), pp. 1–6.
- ¹¹A. P. Bhatnagar and B. Nema, "Conventional and global maximum power point tracking techniques in photovoltaic applications: A review," *J. Renewable Sustainable Energy* 5(3), 032701 (2013).
- ¹²M. Villalva, J. Gazoli *et al.*, "Modeling and circuit-based simulation of photovoltaic arrays," in *Power Electronics Conference (COBEP'09)*, Brazilian (IEEE, 2009), pp. 1244–1254.
- ¹³F. A. Inthamoussou, H. D. Battista, and R. J. Mantz, "New concept in maximum power tracking for the control of a photovoltaic/hydrogen system," *Int. J. Hydrogen Energy* 37(19), 14951–14958 (2012).
- ¹⁴CONNEXA Energy, 2013, Datasheet of bp115 solar module, See <http://bit.ly/K1tY3p>.
- ¹⁵M. Boztepe, F. Guinjoan, G. Velasco-Quesada, S. Silvestre, A. Chouder, and E. Karatepe, "Global mppt scheme for photovoltaic string inverters based on restricted voltage window search algorithm," *IEEE Trans. Ind. Electron.* 61(7), pp. 3302–3312 (2014).